# Effects of Cumulus Convection on the Structure and Growth of the Mixed Layer over South Florida

RICHARD H. JOHNSON

*National Hurricane and Experimental Meteorology Laboratory, NOAA, Coral Gables, Fla. 33124*

(Manuscript received 20 January 1977, in revised form 12 March 1977)

ABSTRACT

Composites of rawinsonde observations of the subcloud layer over south central Florida obtained during the 1975 Florida Area Cumulus Experiment are presented. At a single location south of Lake Okeechobee three soundings per day were released, whenever possible, at approximately 1000, 1300 and 1600 LST during July and August. Soundings have been stratified according to the state of the weather in the vicinity of the release site and time of day. Weather conditions over the south Florida peninsula during the summer period normally ranged from undisturbed (no convective activity) in the morning to highly disturbed (intense convection with precipitation downdrafts) during the afternoon.

Analysis of 47 soundings that ascended into clear air shows rapid growth of the mixed layer beginning 2–3 h after sunrise until shortly before noon, the approximate time of the onset of convective precipitation downdrafts over the peninsula. From the application of simple mixed-layer theory, it is evident that significant subsidence within the cloud environment compensating the net cumulus mass flux occurs on the mesoscale (~10–100 km). The maximum environmental sinking occurs several hours before the time of the heaviest peninsula-scale rainfall, indicating that the intensity of cumulus downdrafts relative to updrafts increases as the convective activity increases during the day. The subcloud layer structure for a number of soundings that ascended into the bases of nonprecipitating cumuli is also examined.

## 1. Introduction

Observations of the structure and properties of the undisturbed tropical oceanic or trade wind atmosphere have been well documented for some time (see review by Garstang and Betts, 1974). Above a relatively shallow, slightly unstable surface layer (0–100 m) there usually exists a neutrally stratified mixed layer approximately 600 m deep. Both potential temperature and mixing ratio are nearly constant in this layer. A roughly isothermal transition layer about 100 m thick normally separates the mixed layer from a cumulus layer above. Recent findings from both aircraft measurements (LeMone and Pennell, 1976) and budget studies (Holland and Rasmussen, 1973; Esbensen, 1975; and others) in the undisturbed trades indicate significant enhancement of the mixed or subcloud layer water vapor fluxes in regions occupied by cumulus clouds over those in clear areas. During disturbed weather conditions the effects of cumulus convection on the subcloud layer structure are even more pronounced. Marked stabilization of the lower troposphere in regions affected by cumulonimbus downdrafts and precipitation has been consistently found (Garstang, 1967; Zipser, 1969; Echternacht and Garstang, 1975; Seguin and Garstang, 1976; Betts, 1976a; Johnson, 1976). In addition, compensating subsidence in the environment of cumulonimbus clouds has been found to significantly influence the depth of the mixed layer on both the cloud scale (e.g., Simpson, 1975) and larger scales (Sarachik, 1974).

Over tropical continental regions observational studies of cloud-subcloud layer interactions are rather limited (Garstang and Betts, 1974; Betts *et al.*, 1974; Betts, 1976a,b). Measurements reported by Garstang and Betts (1974) taken from experiments in Venezuela indicate that in undisturbed conditions the mixed layer structure over continental regions differs to some extent from that observed over the ocean. Approximately the lower one-fourth of the depth of the mixed layer is slightly unstable, while above the structure is slightly stable. Betts (1976a) has determined that a rather consistent transformation of the tropical subcloud layer over Venezuela occurs following the passage of westward moving squall lines to a structure that is nearly well mixed in saturation equivalent potential temperature. In view of the scarcity of observations such as these and those shedding light on the effects of moist convection on the mixed layer depth, it is evident that additional measurements will be necessary to provide an observational basis for the development of mixed layer models applicable to all weather situations over both ocean and land. This paper reports on a series of rawinsonde observations over a subtropical continental region (south central Florida) that are used to examine several aspects of the modification of the subcloud layer by cumulus convection.

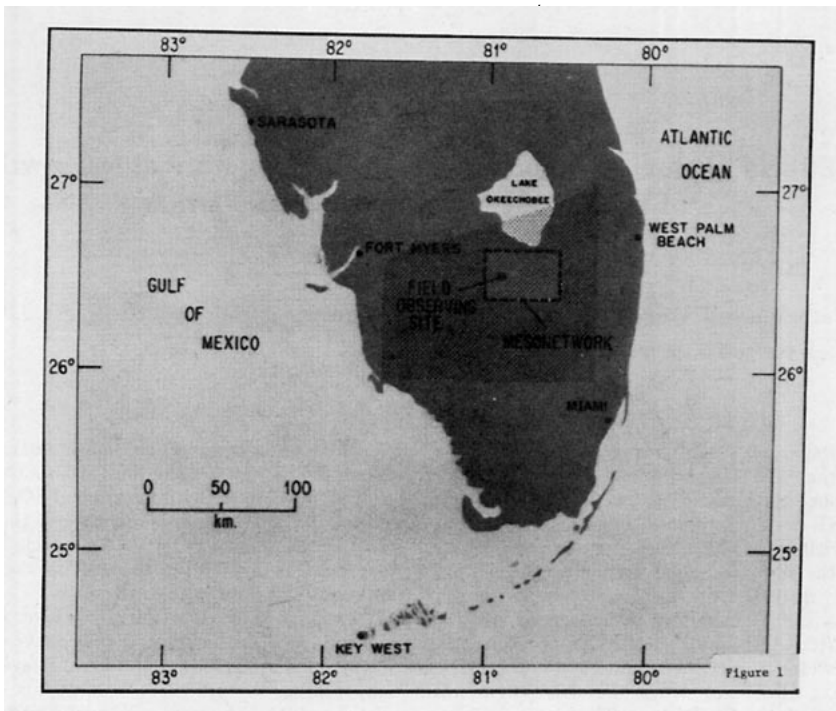


FIG. 1. Site of 1975 Florida Area Cumulus Experiment including mesonetwork area and Field Observing Site, where rawinsondes were released. The stippled region indicates the area in which rainfall rates were determined based on Miami WSR-57 radar data and mesonetwork raingage measurements. FOS is at 26° 34′N, 80° 54′W.

## 2. The measurement program

The observations used in this study were taken during the Florida Area Cumulus Experiment (Simpson and Woodley, 1975; Staff, Cumulus Group, NHEML, 1976) carried out from 16 June to 15 September, 1975. The site of the experiment was just south of Lake Okeechobee (Fig. 1). This region, consisting primarily of everglades and sugar cane fields, is essentially flat (mean elevation $\lesssim 3$ m). A dense surface network of meteorological instruments was established in a 34 km$\times$48 km rectangular area (mesonetwork, Fig. 1) to record wind, pressure, temperature, relative humidity and rainfall during the summer field program. Fifty recording raingages were set up in a 15 km$\times$32 km array (approximate separation 3 km) in the interior of the mesonetwork. An additional 16 raingages were located within the remainder of the mesonetwork for the months July and August. At a single location, the Field Observing Site (FOS), facilities were established for the tracking of rawinsonde balloons. Three rawinsondes per day were released, whenever possible, at 1000, 1300 and 1600 (all times local standard) during July and August. Through cooperation with the U. S. GATE Project Office in Rockville, Md., a large number of GATE omegasondes, series VIZ 1232-300, were acquired for the experiment (see Table 1). In addition, a smaller number of conventional rawinsondes, series VIZ 1295-400, were used. Both sondes had shielded hygrister elements designed to eliminate solar radiation errors present with earlier instrumentation (e.g., Morrissey and Brousaides, 1970).

Balloons with omegasonde transmitters provided a nearly continuous record of temperature and relative humidity having $\sim$1.5 mb resolution in the lower troposphere. The vertical resolution of the conventional radiosonde data is somewhat less ($\sim$10 mb). Significant level data were extracted from the omegasonde strip chart records in a way that provided an effective resolution on the order of 10 mb. Significant levels were selected so that a linear variation between successive values of temperature and relative humidity restricted deviations from observed values in the interval to less than 0.5 K and 5%, respectively. A check on the validity of this approach on a subset of 13 soundings that ascended into the base of nonprecipitating cumuli showed that this method reproduced results obtained by extraction at 10 mb intervals very accurately within the subcloud layer (see Fig. 3 for a comparison for composited soundings). Thermal time constants of the thermistor and hygrister of 5 s and 15–20 s, respectively, for the GATE sensors as reported by Williams and Acheson (1976) imply systematic errors in the subcloud temperature and relative humidity of $\sim+0.2$ K and $\sim-4\%$. In determining these values, average ascent rates for the omega and conventional sondes in the lower troposphere based on all releases away from

cumulus clouds, of 4.3 and 4.6 m $s^{-1}$, respectively, are used. Corrections for thermal lags of the sensors have not been made. Consequently, estimates of cloud-base height, which are determined from the relative humidity traces, will be systematically overestimated by 70–90 m (~7–9 mb) as in Betts (1976a). However, since in this study emphasis is given to subcloud layer structure and growth of the mixed layer, neglect of the above systematic errors will not have a significant effect on the results. In contrast with earlier experiments (e.g., Betts *et al.*, 1974), the response of GATE hygristers above 90% RH is good (Williams and Acheson, 1976), in-cloud relative humidities were generally in the range 95–100%.

Wind measurements from the omega tracking system were not successful due to signal transmission difficulties. Only a scant number of mid- to upper tropospheric wind soundings were obtained. Balloons were tracked at low levels by theodolite; consequently, the subcloud layer wind field was recovered in most cases. Wind records from the surface mesonetwork were not used in this study.

Comprehensive ground-based photographic documentation of the sky conditions at the FOS was obtained during the experiment. Still-camera photographs of the entire horizon at 30 min intervals were used as an aid in determining the degree of convective activity at rawinsonde release time.

## 3. Growth of the mixed layer

### *a. Large-scale controls*

During summer, south Florida characteristically experiences intense afternoon convective activity as a result of sea breeze circulations due to land-ocean differential heating (Byers and Rodebush, 1948; Gentry and Moore, 1954; Frank *et al.*, 1967). Both observations and sea breeze numerical modeling results (e.g., Pielke, 1974) indicate that convection normally occurs in lines related to low-level convergence having orientations largely determined by the synoptic-scale wind field and coastal geography. The intensity of convective activity at any particular location over the peninsula is, therefore, highly dependent on the synoptic-scale flow.

As the land heats and the sea breeze circulation develops during the course of the day, advection of cooler oceanic air modifies subcloud layer air properties and the mixed layer depth, to the greatest extent near the coastline. The question of whether or not FOS is sufficiently distant from the coast (~100 km) to experience negligible oceanic modification under typical wind flow conditions will be examined in the course of the study.

The south Florida sea breeze circulation is complicated by Lake Okeechobee. Direct observations and Pielke's modeling results indicate the presence of subsiding air over the lake in the afternoon, as well as occasional enhancement of convection around the lake coastline due to the development of a lake breeze convergence zone. Those days during which FOS, located ~20 km from the south shore of the lake, was under the influence of the lake breeze have been excluded in the following analysis.

TABLE 1. Number of soundings in each category of subcloud layer structure and sounding type.

| | Time (LST) | | | |
|---|---|---|---|---|
| | 1000 | 1300 | 1600 | Total |
| Subcloud layer structure | | | | |
| Well mixed | | | | |
| Into clear air | 18 | 20 | 9 | 47 |
| Into cloud base | 6 | 7 | 2 | 15 |
| Near cumulonimbi | 0 | 5 | 1 | 6 |
| Not well mixed | | | | |
| Downdraft-influenced | 0 | 10 | 23 | 33 |
| Others | 19 | 7 | 2 | 28 |
| Totals | 43 | 49 | 37 | 129 |
| Sounding type | | | | |
| Omegasonde | 37 | 36 | 19 | 92 |
| Conventional | 6 | 13 | 18 | 37 |

### *b. Composite structure*

From 1 July to 31 August, 129 successful radiosonde balloon launches (several more if dual or multiple launches at some of the observation times are included) were achieved. A breakdown of the releases by time and type of sounding is presented in Table 1. Note that the majority of the sondes (71%) were of the omegasonde type.

A total of 53 soundings passed through a well-mixed layer capped by an inversion, but did not penetrate the base of cumulus clouds. Out of this total, 47 were taken at least 15 km distant from any cumulonimbus clouds. In most of these cases either no cumulonimbi were prevent over the south Florida peninsula or any that were present were >50 km from FOS. The cloud cover within 15 km was predominantly scattered cumulus or cumulus humilis with an average area coverage <0.2 (20%). Incidences when stratiform cloud cover exceeded 0.2 were not included in this category. Most of these soundings (38) occurred at or before 1300, indicating the normally enhanced degree of convective activity that exists later on in the afternoon.

A group of 15 soundings showing a well-mixed layer structure ascended into the bases of nonprecipitating cumulus clouds. In these cases the relative humidity reached a value at or near 100% at the top of the mixed layer (this level was assumed to be cloud base), remaining nearly constant above for an average depth of 450 m. This depth is less than the average of the individual cloud depths, which could not be determined from the experimental data. Ground-based visual estimates of maximum cloud depths within the vicinity

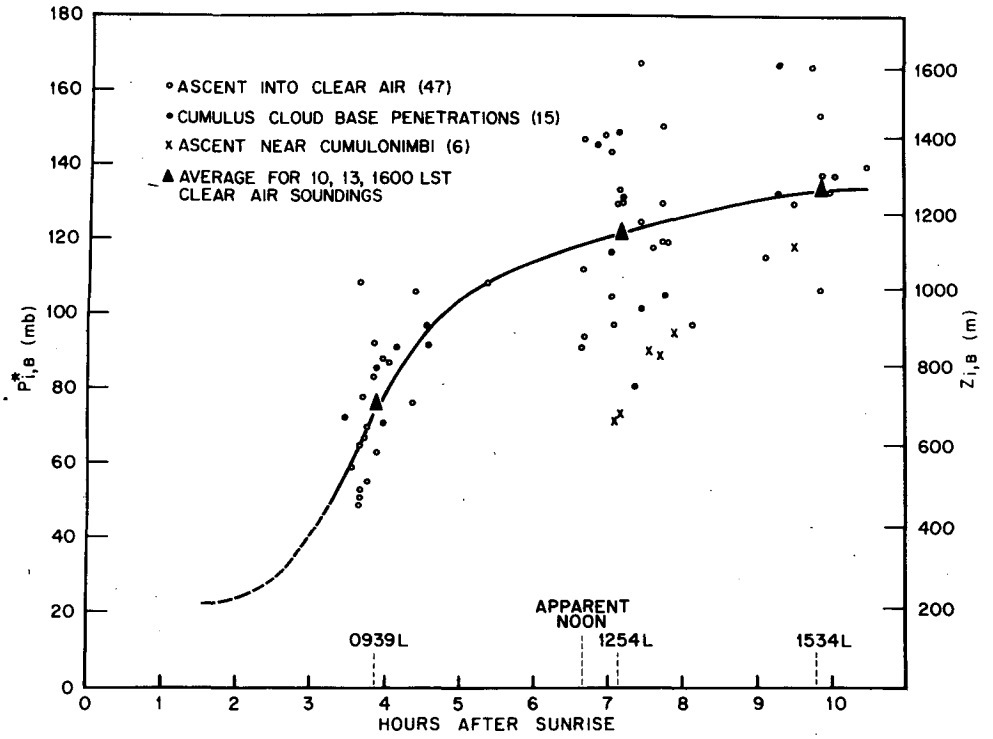


FIG. 2. Variation of the inversion height $p_i^*$, $z_i$ or cloud-base height $p_B^*$, $z_B$ with time for the 68 soundings having a well-mixed layer. The curve in the figure drawn through the average heights for the three time groupings of clear air soundings has been subjectively determined. Number of soundings in each category are indicated in parentheses.

of FOS for this group of soundings are 2000 and 5000 m at 1000 and 1300, respectively.

A small number of soundings (6) ascended through a well-mixed layer in the immediate vicinity of cumulonimbus clouds. All releases in this category were within 13 km of the nearest cumulonimbus cell, the average distance being 6 km. The remaining 61 soundings were either influenced by precipitation downdrafts (33 cases) or did not show a well-mixed structure for other reasons (28 cases).

In Fig. 2 the mixed layer depths for 68 soundings in the three well-mixed categories are shown as a function of time after sunrise. As indicated in the figure the releases were clustered about three central or average times, 0939, 1254 and 1534. Here $z_i$, $p_i^*$ denote the inversion level (top of the mixed layer) for balloons that ascended through clear air and $z_B$, $p_B^*$ denote cloud-base level for ascents into cumulus clouds. Here $p^* \equiv p_s - p$ denotes pressure below the surface pressure $p_s$. The average inversion heights for the 47 clear air soundings are 685, 1147 and 1266 m at 0939, 1254 and 1534 LST, respectively. The curve in the figure passing through these points was subjectively determined. The average inversion level at sunrise was estimated from 1200 GMT (0700 LST) Miami soundings to be approximately 150–200 m.

The growth of the mixed layer as indicated in Fig. 2 resembles that determined in a number of other observations over continental regions: the Great Plains field experiment near O'Neil, Nebr. (Lettau and Davidson, 1957), the Australian Wangara field experiment near Hay (Clarke *et al.*, 1971) and acoustic echo sounder and radar measurements near Wallops Island, Va. (Noonkester, 1976). The above observations were made during weather conditions characterized by an absence of cumulus convection. In contrast, the 47 Florida soundings were released at times when cumulus clouds were nearly always present, ranging in size from a few hundred meters depth for the earliest releases to several kilometers depth during the afternoon. Nevertheless, the rather rapid period of growth of the mixed layer during mid-morning hours seen in other experiments—e.g., Wangara—and discussed in the mixed layer theory of Tennekes (1973) is also evident in this composite of Forida soundings. In the absence of large-scale subsidence a reduction in the growth of the mixed layer would be expected near or shortly after noon (Tennekes, 1973). The growth of the inversion slows markedly shortly before noon, however, and remains small during the afternoon. This behavior is conceivably in response to cumulus convection—specifically, the compensating subsidence that occurs between clouds. The effects of subsidence in the cumulus environment on the development of the mixed layer will be examined by means of a simple model in the next section.

The 15 soundings that ascended into nonprecipitating

cumulus clouds had cloud-base heights that did not vary in any systematic way from the inversion height curve for the clear air soundings (Fig. 2). Slightly larger values for the cloud base height might reasonably be expected considering the fact that the transition layer depth, the distance between the mixed layer top and the cloud layer, is normally on the order of 100 m (10 mb).

Finally, in Fig. 2 we call attention to six balloons that were released in the proximity of cumulonimbus clouds (~6 km away on the average). The distances from FOS to the nearest shower at release time were determined from mesonetwork recorded rainfall data with the aid of photographic data. It is quite apparent that the mixed layer experiences significant suppression in the immediate vicinity of cumulonimbi. This finding is consistent with the theoretical study by Lilly (1960) which concluded that most of the compensating subsidence in areas surrounding moist convective ascent occurs immediately adjacent to the updrafts [for a review of this topic see Fritsch (1975)]. Actual subsidence rates cannot be directly determined from the data in this study. However, from the mixed layer model developed in the following section, it can be indirectly inferred that subsiding motions at cloud base at least as great as 0.5 m $s^{-1}$ must have occurred to produce the mixed layer depths that were observed in the vicinity of cumulonimbus clouds.

Composite subcloud layer values of potential temperature and specific humidity for soundings centered around 1000 and 1300 are presented in Fig. 3. Both clear air and cloud penetration soundings are plotted in the same diagram for the sake of comparison. The vertical axis $\hat{p}$ is a scaled pressure coordinate defined by

$$\hat{p}=\frac{p_s-p}{p_s-p_{i,B}},$$

where $p_i$, $p_B$ are the inversion, cloud-base pressures, respectively; $\hat{p}=1.0$ designates the top of the mixed layer for the clear air soundings and cloud-base height for the cloud penetration soundings. As was mentioned earlier, data were extracted from radiosonde strip charts based on significant level criteria. A comparison of results obtained by this method with those from data extraction from the same soundings at 10 mb intervals for the sondes that passed through cloud base is shown in Fig. 3. Within the subcloud layer the average differ-

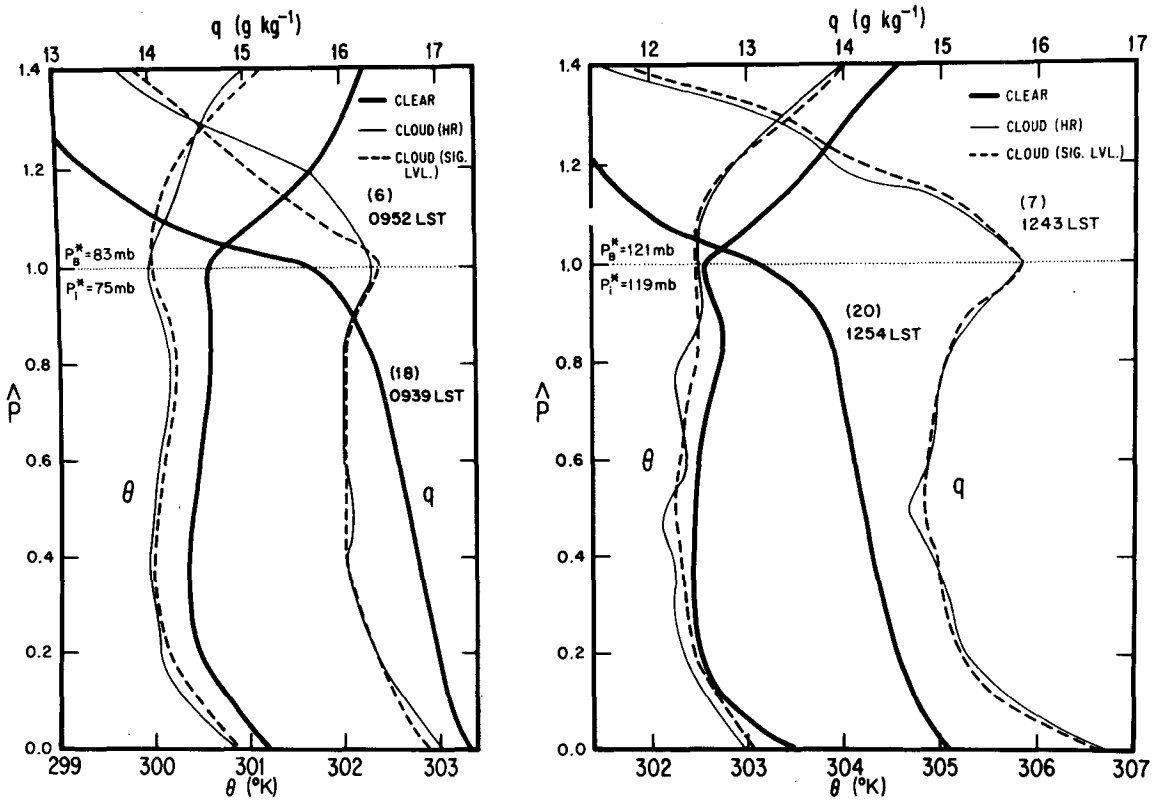


FIG. 3. Mixed-layer potential temperature (K) and specific humidity (g $kg^{-1}$) for composites of clear air soundings and those that ascended into cloud base in the morning and early afternoon. The vertical coordinate $\hat{p}$ is the pressure below the surface pressure scaled by the pressure-depth of the mixed layer or subcloud layer. HR denotes data with ~10 mb vertical resolution. SIG. LVL. refers to composites based on radiosonde data extraction according to the significant level criteria discussed in the text. Number of soundings in each category are indicated in parentheses.

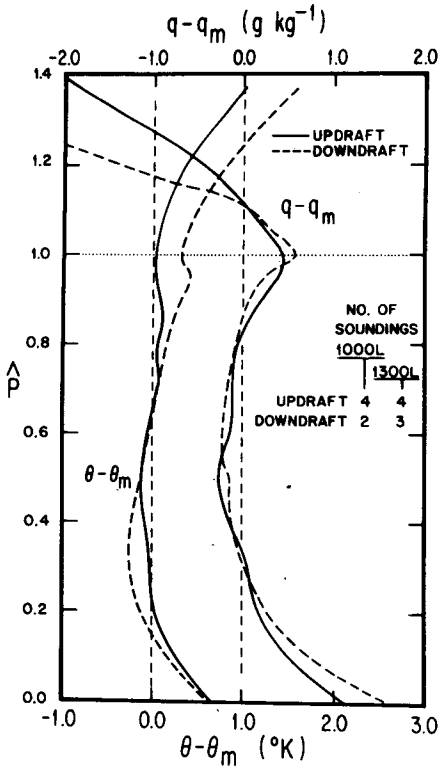


FIG. 4. Potential temperature and specific humidity differences from the mixed-layer mean values for 13 nonprecipitating cloud-penetration soundings. Eight sondes ascended into updrafts and five into downdrafts as determined from the balloon ascent rates.

ences in $\theta$, $q$ are $\sim$0.1 K, 0.1 g kg$^{-1}$. Based on this comparison, we conclude that the significant level method applied to the 129 soundings is sufficiently accurate for the purposes of this study.

Both the morning and early afternoon composite show similar vertical structures of $\theta$ and $q$. The profiles closely resemble those reported by Betts *et al.* (1974) for Venezuelan data. The minimum in $\theta$ at $\hat{p}\approx 0.35$ was also evident in their results. The minor minimum in $\theta$ at $\hat{p}=1$ at 1254, a feature present in many of the 20 soundings at this time, has no apparent explanation. Examination of individual soundings shows that while the mean values of $\theta$ and $q$ within the mixed layer may vary significantly from one sounding to another, the shape of the profiles is usually preserved. The specific humidity decreases gradually through the depth of the mixed layer from $\hat{p}=0.2$ to $\hat{p}=0.8$ and then more rapidly from $\hat{p}=0.8$ to $\hat{p}=1.0$. This behavior has also been observed over Venezuela as reported in a recent paper by Betts (1976b). Mahrt (1976) has given several possible explanations for the decrease with height of the mixed layer specific humidity, which he also observed over the high plains of Colorado during late spring and early summer periods of 1972–74. He argues that entrainment of dry air from above into the mixed layer can explain the observed decrease through the entire mixed layer depth only if the mixed layer growth rate is very large. However, for the south Florida data approximately the same structure is observed at 1254 when the growth rate is small as at 0939 when the growth rate is large, thus making this explanation inadequate, at least for the region $0.2<\hat{p}<0.8$. Undoubtedly entrainment of drier air from aloft accounts for the rapidly varying specific humidity from $\hat{p}=0.8$ to 1.0. It may be that the mean subsidence in the mixed layer in the region between thermal plumes is sufficiently large to advect dry air from upper portion of the mixed layer downward through the entire mixed layer depth to maintain the observed moisture structure. Differential moisture advection has been ruled out as a possible explanation based on the small horizontal moisture gradients that exist in this subtropical region. As a measure of the statistical variation of the structure for all soundings, standard deviations of $\theta-\theta_m$ and $q-q_m$($\sigma_{\theta-\theta_m}$ and $\sigma_{q-q_m}$) at all levels in the mixed layer have been computed. Here $\theta_m$ and $q_m$ are vertically averaged values of $\theta$ and $q$ from $\hat{p}=0.2$ to $\hat{p}=1.0$. The mean or vertically averaged values of $\sigma_{\theta-\theta_m}$ and $\sigma_{q-q_m}$ for the mixed layer are $\pm$0.3 K and $\pm$0.5 g kg$^{-1}$, respectively.

The mixed layer potential temperature structure for soundings that ascended into cumulus bases is similar to that for the clear air soundings. However, the specific humidity profiles differ considerably. A maximum of $q$ within the mixed layer occurs at $\hat{p}=1$, most pronouncedly at 1243 LST. In the work of Betts *et al.* (1974), a peak in $q$ was found at $\hat{p}\approx 0.7$. It is felt that the improved response of the hygrister to relative humidities $>90\%$ for the sondes used in this experiment accounts for the difference in the two results. The elevated specific humidities at cloud base above the mixed layer means suggests that some clouds have origins or roots extending down to the surface layer. The more pronounced peak in $q$ at cloud base at 1243 than at 0952 may indicate that a larger fraction of cumulus clouds have roots within the surface layer in the early afternoon when the clouds are deeper than in the morning when they are very shallow.

The above soundings have been further stratified according to whether or not they ascended into cloud updrafts or downdrafts. This determination is based on the deviation of individual balloon ascent rates from the means for the 47 clear air soundings. Out of 13 releases at $\sim$1000 and 1300, 8 went into cloud updrafts with an average base at 917 mb and 5 into cloud downdrafts with an average base of 911 mb. The average surface pressure was 1018 mb. The variation of $\theta-\theta_m$ and $q-q_m$ within the subcloud layer has been separated into updraft and downdraft averages in Fig. 4. The vertical resolution of the data from these soundings is $\sim$10 mb ($\hat{p}\approx 0.1$). Here the mixed layer means for the updraft soundings do not necessarily represent the actual mean properties of the entire depth of the updraft columns within the subcloud layer nor

do they represent the mean properties of the mixed layer in the region between clouds. Due to vertical wind shear in the subcloud layer, which varied considerably from one sounding to the next, the balloon trajectories very likely extended through only a portion of the updraft roots in many cases. At cloud base ($\hat{p}=1$) $q-q_m\approx 0.5$ g kg$^{-1}$ for both updrafts and downdrafts, whereas $\theta-\theta_m\approx 0$ for updrafts and $\approx 0.3$ K for downdrafts. Differences between updraft and downdraft averages are not statistically significant because of the small number of cases. The average virtual potential temperature difference at the base of the updrafts $\theta_v-\theta_{vm}$ is $\sim 0.1$ K, where $\theta_v=\theta(1+0.61q)$ and $\theta_{vm}$ is the mixed layer mean virtual potential temperature. The average standard deviations of $\theta-\theta_m$ and $q-q_m$ in the mixed layer are $\pm 0.3$ K and $\pm 0.2$ g kg$^{-1}$, respectively.

Further evidence of cloud roots extending down to the surface layer is seen in the variation of the lifting condensation level (LCL) within the mixed layer (Fig. 5). Although the average profile for the eight updraft soundings suggest that cloud base air must have its origins within the surface layer, four of the soundings have LCL maxima within the interval $0.2<\hat{p}<0.5$. The cloud base LCL is less than the average estimated cloud base level because the average cloud-base relative humidity (RH) is only 97% (see Fig. 5). Corrections for thermal lag of the hygrister would probably increase this value to near 100% (Williams and Acheson, 1976).

The average vertical velocity profiles for updrafts and downdrafts are also presented in Fig. 5. The extension of downdrafts to $\hat{p}=0.7$ is due predominantly to the deeper cloud circulations that existed in the early afternoon. Simpson (1975) has reported on observations taken during GATE that indicate that cumulus downdrafts first extend all the way to the surface with the onset of precipitation.

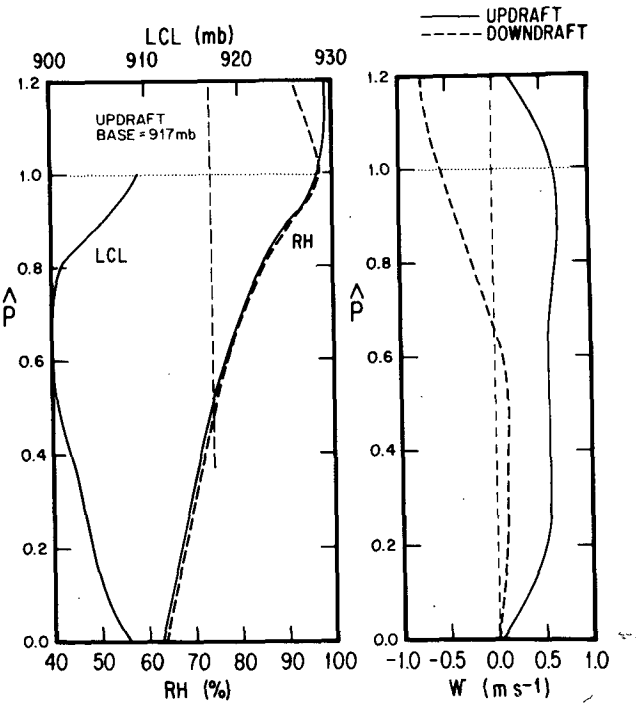


FIG. 5. Mixed layer lifting condensation level LCL(mb) for eight soundings that ascended into cumulus updrafts. Also shown are the relative humidity RH and the vertical velocity $w$(cm s$^{-1}$) along the balloon trajectories for the updraft and downdraft soundings.

## 4. Model for mixed layer growth

We will consider a simplified two-dimensional model for a mixed layer that is capped by a layer of cumulus clouds (Fig. 6). The model is intended to apply to the weather conditions that existed in the vicinity of the 47 clear air soundings—namely, mostly scattered, nonprecipitating cumulus clouds covering a small fraction of the total area. In the following analysis the overbar denotes a horizontal average over a mesoscale area large enough to contain a population of cumulus clouds that is statistically representative of the convective field as described above, yet small compared to the total area. The tilde will refer to values in the cumulus environment within the mesoscale area defined above. Horizontal advective effects are included by imposing an easterly current in the subcloud layer, a situation frequently, though not always, observed during the 1975 experiment. It is assumed that above a superadiabatic surface layer there exists a well-mixed layer with a vertically constant virtual potential temperature $\bar{\theta}_v$. In the region between clouds, hereafter referred to as the cloud environment, the mixed layer is separated from a cumulus layer above by a thin transition layer with a virtual potential temperature jump $\Delta\theta_v\equiv\tilde{\theta}_v(z_B)-\bar{\theta}_v$. The close agreement between cloud base height and inversion height that was found for the 15 cloud-base penetration soundings (Section 3) supports the application of the model to this data set.

In the cloud environment the heat balance across the transition layer from the top of the mixed layer $z_i$ to cloud base $z_B$ yields in the limit $z_B-z_i\to 0$

$$\frac{\partial z_i}{\partial t}-\tilde{w}+u\frac{\partial z_i}{\partial x}=-\frac{(\widetilde{\theta_v'w'})_i}{\Delta\theta_v}, \tag{1}$$

where $\tilde{w}$ is the vertical velocity in the cloud environment, $u$ is the east–west component of the wind, taken to be independent of $x$ and $z$, and $(\widetilde{\theta_v'w'})_i$ is the virtual potential temperature flux at $z_i$ in the cloud environment. It is assumed that there is no jump in the radiative flux across the transition layer. Further, we restrict horizontal variations to the $x$ direction only.

Integration of the equation for $\bar{\theta}_v$ in the mixed layer

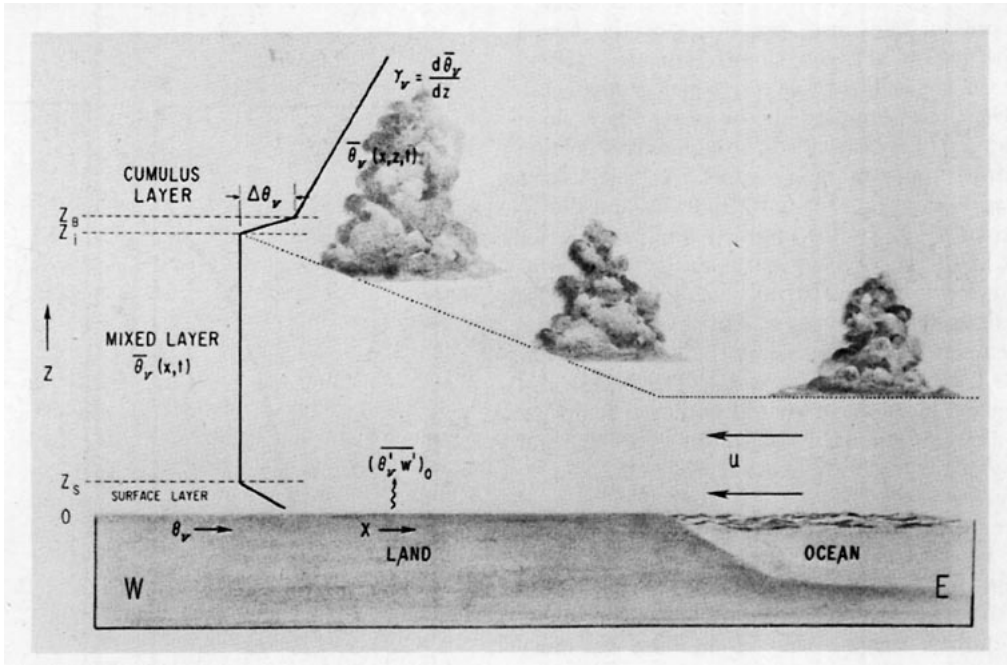


FIG. 6. Model for the mixed layer over south Florida. Symbols are discussed in text.

from $z_s$ to $z_i$ gives

$$\frac{\partial \bar{\theta}_v}{\partial t}=-\frac{1}{\Delta z}[(\overline{\theta_v' w'})_s-(\overline{\theta_v' w'})_i]-u\frac{\partial \bar{\theta}_v}{\partial x}+Q_R, \qquad (2)$$

where $\Delta z=z_i-z_s$, $Q_R$ is the mixed layer mean radiative heating rate, $(\overline{\theta_v' w'})_s$ is the buoyancy flux at $z_s$ and $(\overline{\theta_v' w'})_i$ is the flux of $\theta_v$ at $z_i$ due to the combined effects of turbulent eddies and cumulus roots. Esbensen (1975) has discussed the importance of separately specifying the cumulus and noncumulus eddies at the top of the mixed layer. The contribution to $(\overline{\theta_v' w'})_i$ due to cumulus clouds is determined in a manner similar to that used by Ogura and Cho (1974). Although there seems to be some ambiguity on this matter (Deardorff, 1975), the cumulus contribution to $(\overline{\theta_v' w'})_i$, since it affects $\bar{\theta}_v$, should be evaluated just below the base of the transition layer.

If we represent the nonprecipitating cloud field by a spectrum of cloud sizes (after Arakawa and Schubert, 1974) ranging in size from several meters depth to 1–2 km depth with each cloud having a fractional mass entrainment rate $\lambda$, then the buoyancy flux at $z_i$ can be written as

$$\rho(\overline{\theta_v' w'})_i=M_{ui}[\theta_{vu}(z_i)-\bar{\theta}_v]+\int_0^{\lambda(z_i)} m_d(\lambda,z_i)[\theta_{vd}(\lambda,z_i)-\bar{\theta}_v]d\lambda+\rho(\overline{\theta_v' w'})_i, \qquad (3)$$

where $\rho$ is the air density. Each cloud is assumed to have an updraft and downdraft and both contribute to the flux at $z_i$. Details of the cloud model can be found in Johnson (1976). The first term on the right-hand side of (3) is the transport of $\theta_v$ at $z_i$ due to all updrafts; $M_{ui}$ is the total updraft mass flux at $z_i$. Here we have assumed that the updraft virtual potential temperature just below could base, $\theta_{vu}(z_i)$, is the same for all cloud types. The second term represents the downdraft transport of $\theta_v$ at $z_i$ due to all clouds; $m_d(\lambda,z_i)$ is the downdraft mass flux per unit $\lambda$ at $z_i$. In deriving (3) we have assumed that the fractional area occupied by cumulus clouds is small, which implies $\tilde{\theta}_v\approx\bar{\theta}_v$.

At the base $z_B$ of the cumulus layer, assuming the cloud liquid water content to be vanishingly small, the large-scale equation for $\theta_v$ is

$$\frac{\partial \bar{\theta}_v(z_B)}{\partial t}+u\frac{\partial \bar{\theta}_v(z_B)}{\partial x}+\bar{w}\gamma_v=\frac{M_c(z_B)}{\rho}\gamma_v+\int_0^{\lambda(z_B)}\delta_u(\lambda,z_B)[\theta_{vu}(\lambda,z_B)-\bar{\theta}_v(z_B)]d\lambda+Q_R(z_B)+\gamma_v\frac{dz_B}{dt}, \qquad (4)$$

where $\delta_u(\lambda,z_B)$ is the updraft detrainment rate per unit $\lambda$ at cloud base (Johnson, 1977), $M_c$ is the net cumulus mass flux (i.e., the sum of the updraft and downdraft mass fluxes) and $\gamma_v\equiv(d\bar{\theta}_v/dz)_{z_B}$. The detrainment term represents detrainment from the sides of cumulus updrafts. The effects of detrainment from the sides of downdrafts, although neglected, could be included by adding a term analogous to the updraft detrainment term.

Combining (1)–(4) and noting that $\rho\bar{w}=M_c+\rho\tilde{w}$, we get

$$\frac{\partial\Delta\theta_v}{\partial t}=-\frac{(\widetilde{\theta_v'w'})_i}{\Delta\theta_v}\gamma_v+\int_0^{\lambda(z_B)}\delta_u(\lambda,z_B)[\theta_{vu}(\lambda,z_B)-\bar{\theta}_v(z_B)]d\lambda-\frac{1}{\Delta z}\left\{(\overline{\theta_v'w'})_s-(\widetilde{\theta_v'w'})_i-\frac{M_{ui}}{\rho}[\theta_{vu}(z_i)-\bar{\theta}_v]-\frac{1}{\rho}\int_0^{\lambda(z_i)}m_d(\lambda,z_i)[\theta_{vd}(\lambda,z_i)-\bar{\theta}_v]d\lambda\right\}, \quad (5)$$

where it has been assumed that $\partial\bar{\theta}_v/\partial x\approx\partial\bar{\theta}_v(z_B)/\partial x$.

Eqs. (1) and (5) for $z_i$ and $\Delta\theta_v$, neglecting the convective transport, detrainment and advective terms, are equivalent to those given by Betts (1973) and Sarachik (1974).

We now apply the system (1), (5) to the clear-air sounding data. Large-scale observations necessary to determine $M_{ui}$, $m_d(\lambda,z_i)$ and $\delta_u(\lambda,z_B)$ using the model of Johnson (1976) were not available. For the shallow convection present here the terms in (5) containing $M_{ui}$, $m_d(\lambda,z_i)$ are small compared to $(\overline{\theta_v'w'})_s$ for reasonable estimates of cloud-environment differences in $\theta_v$ and cumulus mass fluxes. In Section 3 it was found that $\theta_{vu}(z_i)-\theta_{vm}\approx 0.1$ K, where $\theta_{vm}$ is the vertically averaged virtual potential temperature beneath the cloud along the balloon trajectory. Although this quantity is not the same as $\theta_{vu}(z_i)-\bar{\theta}_v$, it is not unreasonable to expect, considering the above result, that $\theta_{vu}(z_i)-\bar{\theta}_v$ might also be small. Considering the small area occupied by convection in the vicinity of these soundings, we will neglect as a first approximation the effects of cloud detrainment on $\Delta\theta_v$, although measurements are not available to justify this step.

The closure condition

$$(\widetilde{\theta_v'w'})_i=-k(\overline{\theta_v'w'})_0 \quad (6)$$

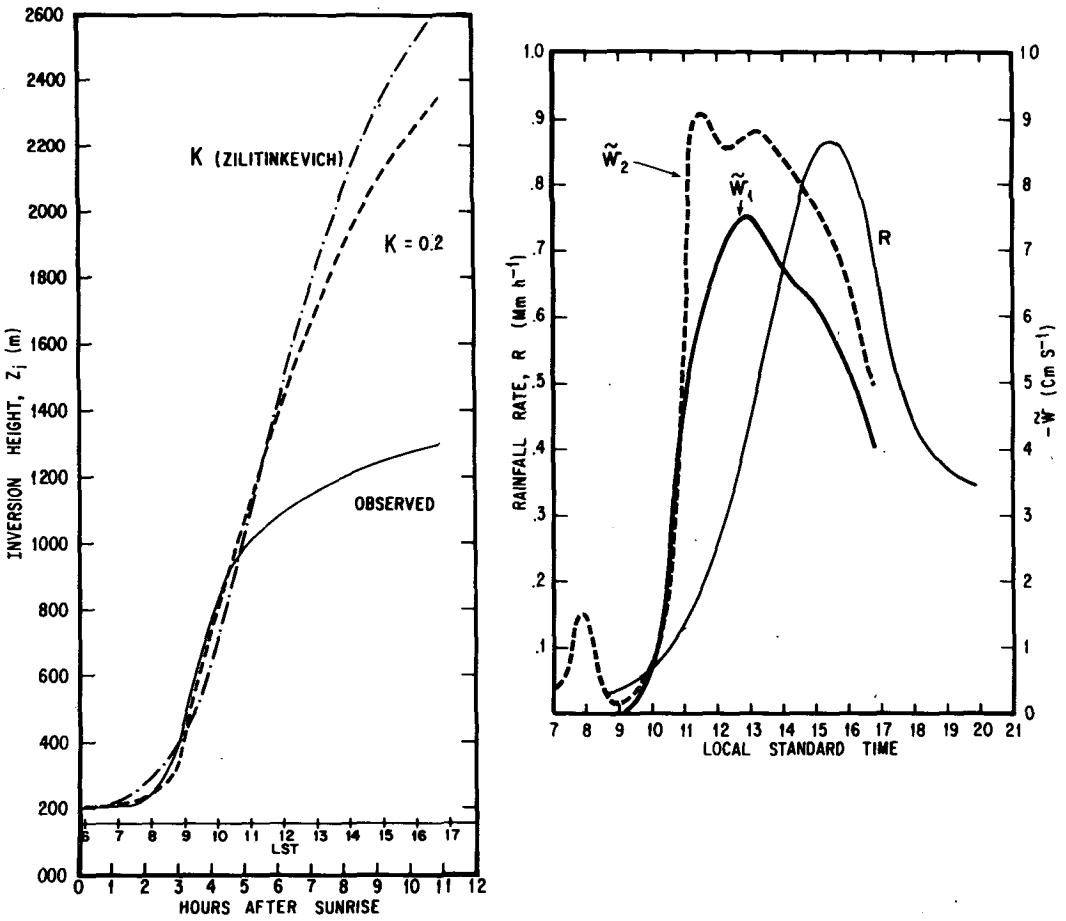


FIG. 7. Observed and predicted growth of the mixed layer (left) for both closure assumptions, $k=0.2$ and $k$ as given by Zilitinkevich (1975); and rainfall rate $R$ (mm h$^{-1}$) and environmental subsidence $\tilde{w}$ (cm s$^{-1}$) as a function of time of day (right). $\tilde{w}_1$ is the result for $k=0.2$ and $\tilde{w}_2$ is that obtained using Zilitinkevich's formulation.

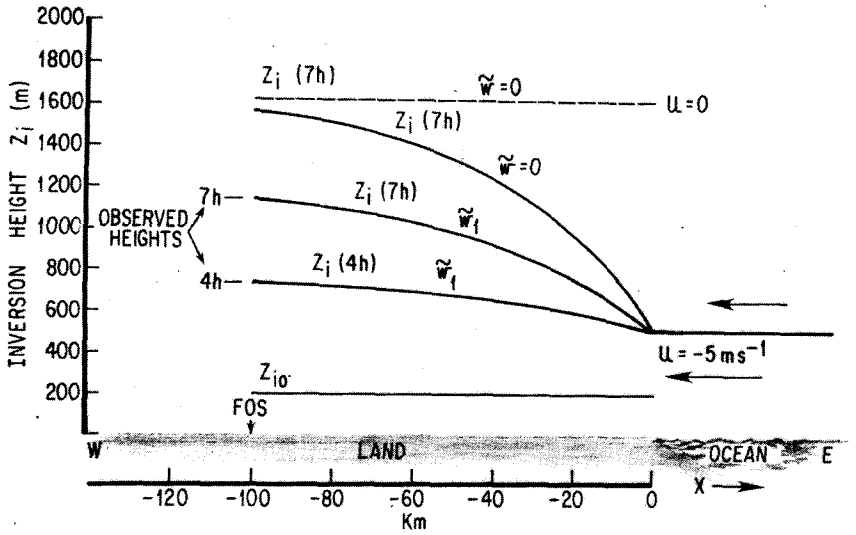


FIG. 8. Variation of mixed-layer depth (m) with distance from ocean (km) for no-wind case ($u=0$) and a 5 m s$^{-1}$ easterly current. Results for $\tilde{w}=0$ and $\tilde{w}_1$ from Fig. 7 are presented. Numbers in parentheses are times (in hours) after sunrise. The initial inversion height over land $z_{i0}$ is 200 m and the equilibrium height over the ocean is 500 m.

is used, where $(\overline{\theta_v' w'})_0$ is the surface buoyancy flux, assumed to be approximately equal to $(\overline{\theta_v' w'})_s$. In the simplest case $k=$constant; however, the form for $k$ derived by Zilitinkevich (1975) that includes the effects of nonstationary of turbulence kinetic energy at the inversion level has also been tested:

$$k=c\left[1+\frac{c_1(\overline{\theta_v' w'})_0^{\frac{1}{2}}}{(gz_i/T_i)^{\frac{1}{2}}\Delta\theta_v}\right]^{-1},$$

where $T_i$ is the temperature at the inversion base.

Eqs. (1) and (5) have been solved for $z_i$, $\Delta\theta_v$ using a fourth-order Runge-Kutta method with a time interval of 30 min. The surface flux has been prescribed by $(\overline{\theta_v' w'})_0 \sin\omega t$, where $\omega=\pi/2\tau$, $\tau=6.75$ h (one-half the time from sunrise to sunset), $t=0$ at sunrise and $(\overline{\theta_v' w'})_0=0.25$ m K s$^{-1}$, a value appropriate for this region of south Florida and mostly clear sky conditions (P. Gannon, personal communication, NOAA, NHEML, Coral Gables, Fla.). The observed lapse rates are

$$\gamma_v=\begin{cases}1.9\times10^{-2}\text{ K m}^{-1}, & 0\leqslant t<3\text{ h}\\ 3.3\times10^{-3}\text{ K m}^{-1}, & 3\leqslant t<5.5\text{ h}\\ 2.9\times10^{-3}\text{ K m}^{-1}, & 5.5\leqslant t\leqslant 11\text{ h}.\end{cases}$$

The value for $t<3$ h was determined from 0700 LST Miami sounding data. We have selected $k=0.2$ and $c=0.5$, $c_1=2.6$ based on Tennekes' (1975) findings. Initial values of $z_i$ and $\Delta\theta_v$ are 200 m and 3 K. Results are insensitive to the choices, within reasonable bounds, of initial conditions as Tennekes (1973), Mahrt and Lenschow (1976) and others have pointed out.

For the case $u=\tilde{w}=0$, the solution for $z_i$ is shown in Fig. 7 for both closure assumptions. The mixed layer depth given by the theory agrees well with the observed up until about 5 h after sunrise ($\sim$1100), beyond which point there is a significant overprediction of $z_i$ for both cases. With Zilitinkevich's formulation, $k$ decreases from 0.48 at $t=0$ h to 0.34 at $t=4$ h and then increases to 0.46 at 11 h. It is clearly evident from these results and Eq. (1) that significant subsidence must occur in the afternoon in the between-cloud environment to account for the observed growth of the inversion. Using the observed variation of the inversion height with time, the system (1), (5) was next solved for $\tilde{w}$. The results of these computations are shown in Fig. 7. For either closure assumption there is clearly a rapid increase in $|\tilde{w}|$ after 1000 to a peak near noon and a subsequent decrease into the afternoon.

Also plotted on the same diagram is the average rainfall rate $R$ over the area enclosed within the $1.3\times10^4$ km$^2$ quadrilateral in Fig. 1. Precipitation rates were determined from quantitative radar measurements using the Miami-based WSR-57 with adjustments based on mesonetwork rainfall in the manner described by Woodley *et al.* (1975). Except for those days in which tropical disturbances were present, $R$ was usually a maximum in the afternoon. From 35 days of data that were available during July and August, it was found that the average maximum R occurred at 1530 LST $\pm$1.8 h, at least 2 h after the maximum environmental subsidence. Since the net cumulus mass flux $M_c\approx-\rho\tilde{w}$ at cloud base when convective activity is strong, this result implies that $M_c$ is a maximum several hours before the peak in $R$. Furthermore, since $R$ is proportional to the updraft mass flux $M_u$ (see, e.g., Johnson,

1976), it must be concluded from these composite results that until about 1300, cumulus clouds consist predominantly of updrafts and thereafter the intensity of cumulus downdrafts relative to updrafts increases. The increase in downdraft activity would naturally be expected to coincide with the rapid increase in R, as inferred in Fig. 7.

The above results are consistent with the idea that the lower troposphere, from the time of the first appearance of shallow cumuli at ~0900 to 1300 when towering cumuli exist, is moistened by repeated growth and dissipation of cumulus clouds having little or no organized downdrafts. Composite soundings of the lower troposphere at 1000 and 1300 (not shown) indicate this moistening effect of the shallow cumuli. Later on, when the clouds are sufficiently deep, precipitation begins and the downdraft intensity increases significantly.

Advective effects on the mixed-layer growth have been examined by imposing a constant flow within the subcloud layer. FOS is approximately 100 km from the Atlantic Ocean, which is assumed to have an equilibrium mixed-layer depth above it of 500 m. The system (1), (5) is solved with initial values of $z_i$ and $\Delta\theta_v$ of 200 m and 3 K over land. The horizontal derivative of $z_i$ is determined using one-sided differences at 10 km intervals working inland from the coastline. The vertical velocity $w$ has been set equal to zero in one case and $\tilde{w}_1$ from Fig. 7 in another. With a constant current of 5 m s$^{-1}$, the growth of $z_i$ is severely restricted near the coastline, but at FOS there is only a 5% reduction in $z_i$ below the no wind ($u=0$) case for $\tilde{w}=0$ at $t=7$ h (Fig. 8). Predicted inversion heights using the earlier solution for $\tilde{w}$ ($\tilde{w}_1$ from Fig. 7) where $k=0.2$ are shown for $t=4$, 7 h. Because the wind flow was not consistently from a single direction during the course of the experiment and significant vertical wind shears frequently existed in the mixed layer, an exact determination of advective effects was not possible for each of the soundings. On occasion, easterly winds as large as 10 m s$^{-1}$ occurred; on these days advective effects may have reduced $z_i$ by 100–200 m in the afternoon at FOS.

## 5. Summary and conclusions

The effects of cumulus convection on the structure and properties of the subcloud layer over south Florida before the onset of precipitation downdrafts have been examined. Rawinsonde observations taken from a single location just south of Lake Okeechobee at approximately 1000, 1300, and 1600 LST during the months of July and August, 1975, have been used in the analysis. Soundings have been stratified according to the weather conditions that existed in the vicinity of the release site at the time of the release. Out of a total of 129 soundings, 68 showed well-mixed layer structure: 47 ascended into clear air, 15 went through the bases of nonprecipitating cumulus clouds and 6 ascended into the clear air near cumulonimbus clouds. The remaining soundings were either influenced by precipitation downdrafts or did not exhibit a mixed layer.

The temperature and moisture structure of the mixed layer during undisturbed conditions for this subtropical continental region during late morning and early afternoon is quite similar to that reported by Betts *et al.* (1974) over Venezuela. The specific humidity decreases slowly with height in the middle to lower portion of the mixed layer and more rapidly near the mixed layer top, probably as a result of entrainment of drier air aloft and strong mean subsidence in the layer. The mixed layer structure beneath nonprecipitating cumulus clouds shows a maximum in specific humidity and lifting condensation level at cloud base, implying that the updraft roots of some cumuli extended to the surface layer, especially in the afternoon.

The observed growth of the mixed layer is predicted quite well by simple mixed layer theory neglecting mean subsidence until approximately 1100, when convective precipitation over the south Florida peninsula begins a rapid increase toward its afternoon maximum at about 1530. Using the observed growth of the inversion, the time dependence of the environmental subsidence has been determined. The maximum environmental sinking occurs several hours before the time of the heaviest peninsula-scale rainfall, indicating that the intensity of cumulus downdrafts relative to updrafts increases as the convective activity increases during the course of the day. A major, unresolved question is the relationship of the mean vertical motion, which could not be determined from the available data, to the convective activity and precipitation. In addition, due to the lack of large-scale observations of the wind field, it was not possible to determine the convective mass fluxes. In particular, the role of convective transports and cloud detrainment in maintaining the inversion could not be determined. These transports become increasingly important as the convection increases in areal coverage and intensity during the course of the day.

*Acknowledgments.* Sincere thanks are extended to Jack Thomas, who, as a result of extensive efforts in planning and implementation of the rawinsonde observation program and follow-up analysis, has provided the data set used in this study. In addition, the assistance of Ron Holle with photographic data has been sincerely appreciated. The author acknowledges helpful discussions with Drs. Stanley Rosenthal and Lloyd Shapiro and Dr. John M. Brown, Iowa State University. Thanks also go to Sally Michalover for her skillful typing of the manuscript and Dale Martin for drafting the figures.

## REFERENCES

Arakawa, A., and W. H. Schubert, 1974: Interaction of a cumulus cloud ensemble with the large-scale environment, Part I. *J. Atmos. Sci.*, **31**, 674–701.

Betts, A. K., 1973: Non-precipitating cumulus convection and its parameterization. *Quart. J. Roy. Meteor. Soc.*, **99**, 178–196.
——, 1976a: The thermodynamic transformation of the tropical subcloud layer by precipitation and downdrafts. *J. Atmos. Sci.*, **33**, 1008–1020.
——, 1976b: Modeling subcloud layer structure and interaction with a shallow cumulus layer. *J. Atmos. Sci.*, **33**, 2363–2382.
——, F. J. Dugan and R. W. Grover, 1974: Residual errors of the VIZ radiosonde hygristor as deduced from observations of the subcloud layer structures. *Bull. Amer. Meteor. Soc.*, **55**, 1123–1125.
Byers, H. R., and H. R. Rodebush, 1948: Causes of thunderstorms of the Florida Peninsula. *J. Meteor.*, **5**, 275–280.
Clarke, R. H., A. J. Dyer, R. R. Brook, D. G. Reid and A. J. Troup, 1971: The Wangara experiment: Boundary layer data. Tech. Pap. No. 19, Div. Meteor. Phys., CSIRO, Melbourne, Australia, 350 pp.
Deardorff, J. W., 1975: Comments "On the interaction between the subcloud and cloud layers in tropical regions." *J. Atmos. Sci.*, **32**, 2363–2364.
Echternacht, K. L., and M. Garstang, 1976: Changes in the structure of the tropical subcloud layer from the undisturbed to the disturbed states. *Mon. Wea. Rev.*, **104**, 407–417.
Esbensen, S., 1975: An analysis of subcloud-layer heat and moisture budgets in the western Atlantic trades. *J. Atmos. Sci.*, **32**, 1921–1923.
Frank, N. L., P. L. Moore and G. E. Fisher, 1967: Summer shower distribution over the Florida Peninsula as deduced from digitized radar data. *J. Appl. Meteor.*, **6**, 309–316.
Fritsch, J. M., 1975: Cumulus dynamics: Local compensating subsidence and its implications for cumulus parameterization. *Pure Appl. Geophys.*, **113**, 851–867.
Garstang, M., 1967: Sensible and latent heat exchange in low-altitude synoptic-scale systems. *Tellus*, **19**, 492–509.
——, and A. K. Betts, 1974: A review of the tropical boundary layer and cumulus convection: Structure, parameterization and modeling. *Bull. Amer. Meteor. Soc.*, **55**, 1195–1205.
Gentry, R. C., and P. L. Moore, 1954: Relation of local and general wind interaction near the sea coast to time and location of air-mass showers. *J. Meteor.*, **11**, 507–511.
Holland, J. Z., and E. M. Rasmusson, 1973: Measurements of the atmospheric mass, energy and momentum over a 500-kilometer square of tropical ocean. *Mon. Wea. Rev.*, **101**, 44–55.
Johnson, R. H., 1976: The role of convective-scale precipitation downdrafts in cumulus and synoptic-scale interactions. *J. Atmos. Sci.*, **33**, 1890–1910.
——, 1977: The effects of cloud detrainment on the diagnosed properties of cumulus populations. *J. Atmos. Sci.*, **34**, 359–366.
LeMone, M. A., and W. T. Pennell, 1976: The relationship of tradewind cumulus distribution to subcloud layer fluxes and structure. *Mon. Wea. Rev.*, **104**, 524–539.
Lettau, H. H., and B. Davidson, 1957: *Exploring the Atmosphere's First Mile*, Vol. 2. Pergamon Press, 578 pp.
Lilly, D. K., 1960: On the theory of disturbances in a conditionally unstable atmosphere. *Mon. Wea. Rev.*, **88**, 1–17.
Mahrt, L., 1976: Mixed-layer moisture structure. *Mon. Wea Rev.* **11**, 1403–1407.
—— and D. H. Lenschow, 1976: Growth dynamics of the convectively mixed layer. *J. Atmos. Sci.*, **33**, 41–51.
Morrissey, J. F., and F. J. Brousaides, 1970: Temperature induced errors in the ML-476 humidity data. *J. Appl. Meteor.*, **9**, 805–808.
Noonkester, V. R., 1976: The evolution of the clear air convective layer revealed by surface-based remote sensors. *J. Appl. Meteor.*, **15**, 594–606.
Ogura, Y., and H. R. Cho, 1974: On the interaction between the subcloud and cloud layers in tropical regions. *J. Atmos. Sci.*, **31**, 1850–1859.
Pielke, R., 1974: A three-dimensional numerical model of the sea breezes over South Florida. *Mon. Wea. Rev.*, **102**, 115–139.
Sarachik, E. S., 1974: The tropical mixed layer and cumulus parameterization. *J. Atmos. Sci.*, **31**, 2265–2230.
Seguin, W. R., and M. Garstang, 1976: Some evidence of the effects of convection on the structure of the tropical subcloud layer. *J. Atmos. Sci.*, **33**, 660–666.
Simpson, J. 1975: On the observational basis of cumulus parameterization. Paper presented at first AMS Conference on Parameterization, Chicago, Ill., 3 December [Available from author, University of Virginia, Charlottesville, Va.]
—— and W. L. Woodley, 1975: Florida area cumulus experiments 1970–73 rainfall results. *J. Appl. Meteor.*, **14**, 734–744.
Staff, Cumulus Group, NHEML, Weather Modification Program Office, 1976: 1975 Florida area cumulus experiment (FACE): Operational summary. NOAA Tech. Memo. ERL WMPO-28, 186 pp. [Available from National Hurricane and Experimental Meteorology Laboratory, Coral Gables, Fla.]
Tennekes, H., 1973: A model for the dynamics of the inversion above a convective boundary layer. *J. Atmos. Sci.*, **30**, 558–567.
——, 1975: Reply to comments on "A model for the dynamics of the inversion above a convective boundary layer." *J. Atmos. Sci.*, **32**, 992–995.
Williams, S. L., and D. T. Acheson, 1976: Thermal time constants of U. S. radiosonde sensors used in GATE. NOAA Tech. Memo. EDS CEDDA-7, 56 pp. [NTIS No. PB 257367/AS].
Woodley, W. L., A. R. Olsen, A. Herndon and V. Wiggert, 1975: Comparison of gage and radar methods of convective rain measurement. *J. Appl. Meteor.*, **14**, 909–928.
Zilitinkevich, S. S., 1975: Comments on "A model for the dynamics of the inversion above a convective boundary layer." *J. Atmos. Sci.*, **32**, 991–992.
Zipser, E. J., 1969: The role of organized unsaturated convective downdrafts in the structure and rapid decay of an equatorial disturbance. *J. Appl. Meteor.*, **8**, 799–814.